RESEARCH ARTICLE

A Geometric Structure Based Non Local Mean Image Denoising Algorithm

LEI SHI

School of Mathematics and Physics, Hulunbuir University, Hulunbuir 021008, China

e-mail: slei0224@163.com

ABSTRACT With the widespread application of image recognition technology, the commercial application value of image denoising is gradually increasing. To optimize the performance of non local mean image denoising algorithms, the similarity of image blocks in this algorithm is now integrated into the evaluation calculation steps of image block direction similarity and geometric information similarity. A neural network structure is used to optimize the mapping function between image blocks, assisting the NLM algorithm in finding the similarity of image blocks. The denoising experimental results for the improved algorithm show that when the noise variance is 25, the normalized peak signal-to-noise ratios of the improved algorithm are 0.58, 0.62, and 0.43, respectively. The improved non local mean image denoising algorithm outperforms other comparative algorithms in terms of information entropy, peak signal-to-noise ratio, and average gradient, which represent the denoising effect. When the noise variance is 45, the normalized structural similarity, mutual information, root mean square error, and absolute error of the algorithm are 0.88, 0.78, 8.2, and 9.7, respectively. The improved non local mean image denoising algorithm performs better than other algorithms in terms of evaluation indicators such as structural similarity, mutual information, root mean square error, and absolute error in preserving original information. It can be seen that the improved algorithm designed in this study has better denoising performance than common methods, and can retain the core information of the original image. It can provide higher quality image denoising services for meteorological prediction, agricultural planting, and other fields.

INDEX TERMS Non local mean image denoising, similarity, noise, directional structure.

I. INTRODUCTION

Image denoising technology belongs to the important research directions in the image processing, aiming to eliminate noise in images and improve image quality and usability [1], [2]. For many image applications, such as medical imaging, remote sensing images, and security monitoring, image noise often affects the reading, recognition, and analysis of images, severely limiting their effectiveness and accuracy in practical applications [3]. Recently, with the continuous advancement of computer science, mathematics, and engineering, non local mean image denoising algorithms (NLMIDA)in view of geometric structures have gradually been a research focus in the image denoising (ID) [4], [5]. The main idea is to denoise the image under the assumption of

geometric structure through non local mean filtering, thereby improving the quality and clarity of the image [6]. In the development process of NLMIDA, numerous model-based and statistical-based ID algorithms have been proposed and gradually applied widely [7], [8]. Among them, model-based algorithms mainly include algorithms based on wavelet transform, nonlinear diffusion, variational, sparse encoding, etc. These algorithms can to some extent handle noise in images, and are often used by scholars to solve various image denoising problems. Ye H et al. found that deep learning technology has high application value in hyperspectral image denoising, so the author team proposed an image denoising algorithm based on deep Convolutional neural network, which uses adaptive regularization parameter criteria and enhances nodes and feature mapping nodes. The test results show that the algorithm has excellent denoising performance in hyperspectral images, and the image quality after denoising

---

The associate editor coordinating the review of this manuscript and approving it for publication was Shuihua Wang.

is higher than the current more advanced image denoising algorithms. However, the denoising performance is poor for non hyperspectral images with a large number of key areas, mainly because there is no attention mechanism structure, which cannot allocate denoising computing resources with a certain focus. Li K et al. designed an image denoising method based on an improved deep neural network, And apply it to binary signal detection tasks. Research has found that the denoised images processed by this deep neural network algorithm can better recover signals, thereby effectively improving detection performance. Compared to traditional methods, this method has better performance and wider applicability. The research results have significant implications for the fields of image processing and signal detection, providing feasible ideas and methods for the research and development of these fields. However, the disadvantage of this algorithm is that there is no significant difference in the denoising effect when processing non binary data compared to the improved algorithm [10]. Li P proposed an image denoising algorithm based on adaptive clustering and Singular value decomposition. The algorithm first uses adaptive clustering to divide the input image into multiple subsets, then Singular value decomposition is performed on each subset, and finally the images are re merged. The experimental results show that this algorithm can effectively remove noise while maintaining image details, and has high peak signal-to-noise ratio and clarity. Compared with other existing image denoising methods, this algorithm has better noise suppression effect and higher computational efficiency, but its denoising effect is poor for images without obvious category features because the adaptive clustering module in the algorithm cannot function properly for such images [11].

It can be seen that although the denoising algorithms and methods proposed by previous people can effectively solve the problems they face, the technical disadvantage or gap of these methods is that their denoising effect is related to the type of image being processed, and in some cases, their denoising ability may be very poor. And algorithms based on statistics, especially those based on non local mean filtering, can not only handle various complex noises, but also have good denoising effects. The main idea is to achieve denoising by finding local image blocks similar to the pixels to be processed, thereby improving the quality and clarity of the image. Algorithms based on non local mean filtering have broad application prospects in practical applications. However, due to the fact that the similarity calculation of the Non Local Means (NLM) algorithm only considers the geometric structure information of the image, it is easy to generate denoising errors and delete some non noise data. Therefore, it is necessary to improve this algorithm. So the main purpose of this study is to design an improved non local mean image denoising algorithm, and explore its superiority and application prospects through experimental analysis.

The overall organization of this study consists of four parts. The first part introduces the background, purpose, and significance of the study. The motivation of this study is to design image denoising methods with superior denoising performance. The core content of the second part is to design a non local mean image denoising algorithm based on improved similarity calculation method and improved edge point detection judgment method, and integrate a special neural network structure designed in this algorithm to optimize the similarity calculation steps of image blocks. This part is also the innovation and scientific contribution of this study.The third part is to conduct denoising experiments using on multiple noisy image datasets, and compare the experimental results with existing artificial intelligence based and statistical ID algorithms. The fourth part is the analysis of the results obtained through testing and calculation.

II. RELATED WORKS

ID technology can provide clearer and high-quality image data for industries such as photography and exploration, which has attracted a large number of scholars' attention. Golshan H proposed a new ID method - fuzzy hysteresis smoothing. This method effectively suppresses the influence of noise and other uncertain factors by clustering image pixels, and improves the PSNR and clarity. The experiment illustrates that this method has higher performance and better applicability compared to traditional ID methods. This algorithm can diminish noise while preserving the original details and textures of the image, and is fast [12].

Jia P believes that autoencoders have certain value in assisting algorithms in identifying noisy data in images, so he has designed an ID algorithm based on autoencoders. This algorithm is used for modelingthe point spread function of a wide-field, small-aperture telescope. This algorithm first trains an autoencoder to learn image noise features, and then applies it to PSF modeling to obtain more accurate image reconstruction. Through experimental verification, this algorithm can markedly enhance the effectiveness of ID and reduce the impact of noise and artifacts. In addition, this algorithm also has good computational efficiency and practicality, and is expected to be more widely applied in practical applications [13]. Lotfi Y's research proposes an efficient technique for ID using meshless methods. The author explores the application of the operator splitting RBF interpolation method in two anisotropic diffusion problems. This method improves the clarity and contrast of the image by effectively handling noise and artifacts in the image. The experiment indicates that this method can effectively remove different types of image noise while preserving image details, with better PSNR and higher computational efficiency. These results indicate that this method has wide application in image processing and can provide important theoretical and practical value to related fields [14]. Riya found that existing ID methods have insufficient accuracy in processing edge information in images, and therefore proposed an efficient anisotropic diffusion model for ID and edge information preservation. This model comprehensively utilizes

tensor operations and spatial gradient information, effectively suppressing noise and smoothing images, while preserving image details and edges. The experiment demonstrates that this method can achieve excellent denoising effects in various noise environments, with high PSNR and better visual effects. Compared with other existing ID methods, this method has higher computational efficiency and better smoothing performance [15]. Han L et al. introduced a non local frame ID algorithm in terms of Gaussian mixture model and its intra-block covariance. In addition, a benchmark dataset for ID was constructed to evaluate the performance of different denoising algorithms. The experiment indicates that the designed algorithm is superior to other existing algorithms in denoising effect and speed, and has good adaptability to images with different noise types and intensities. This dataset provides useful reference for research in ID, and the study of this algorithm also provides new ideas and methods for the development and application of ID algorithms [16].

In summary, although previous researchers have designed various improved models to improve the denoising performance, stability, and computational speed of various ID algorithms, few studies have considered both geometric and directional structural information in the image. The directional structure information in images has important applications in determining noisy pixels in images. Therefore, to improve the denoising ability of denoising algorithms, this study attempts to design a denoising algorithm that can simultaneously consider image geometry and directional information.

III. DESIGN OF A NON LOCAL MEAN IMAGE DENOISING ALGORITHM BASED ON IMPROVED GEOMETRIC STRUCTURE INFORMATION CALCULATION

The NLM denoising algorithm can perform denoising operations by calculating the similarity between image blocks based on the information in the image itself [17]. However, traditional NLM denoising algorithms only consider the geometric structure information between image blocks, and use Gaussian weighting to calculate the Euclidean distance to form similarity indicators, while the directional structure information contained in image blocks is insufficiently considered. This can lead to certain denoising errors, and even consider missing similar image blocks are not taken into account when necessary [18], [19]. Moreover, the filtering parameter values of traditional NLM denoising algorithms are globally fixed, which may lead to poor denoising ability in flat areas of the image or over-smoothing of details. Therefore, to improve the denoising ability of the NLM denoising algorithm, it is necessary to improve its design.The similarity calculation formula for image blocks in traditional NLM algorithms has been improved to reflect both geometric similarity and directional structure information between image blocks. And the edge point detection of the Canny algorithm is used to support the calculation of similarity weights, thus forming an improved NLM algorithm.

A. SIMILARITY CALCULATION METHOD FOR MIXED GEOMETRIC STRUCTURE AND DIRECTIONAL STRUCTURE INFORMATION

The traditional NLM denoising algorithm has isotropy in image similarity calculation, and the angle used for measuring the similarity between image blocks is only the grayscale value of pixels, which cannot reflect other structural information of image blocks. This error is shown in Figure 1 here. The numbers inside the square in Figure 1 represent pixel values [20]. If the traditional NLM denoising algorithm is used to process the image, the similarity of image blocks 2 and 3 relative to image block 1 is consistent, and they will be given the same weight during the denoising process. But image block 2 also contains directional information from image block 1, indicating that image block 2 is the true similar image block to image block 1.

(a) Image block 1 (b) Image block 2 (c) Image block 3

FIGURE 1. Error display of traditional NLM denoising algorithm based on geometric structure information.

To avoid errors caused by the inherent defects of this algorithm, Local Structural Direction Similarity (LSDS) is introduced to improve the similarity computation. The aim is to enable the NLM denoising algorithm to consider both image geometry and directional structure for denoising. The algorithm is designed to extract structural direction information from any point (i, j) in the image, with *len* being the 1/2 neighborhood of that point. If a straight line $L(\theta)$ with an angle of θ passes through the point and its neighborhood *Neigh* is divided into $s1$ and $s2$, then the direction information E of the point can be expressed according to equation (1).

$$M = \max (f_{s2} - f_{s1}) \tag{1}$$

In equation (1), f_{s1} and f_{s2} represent the sum of each pixel in $s1$ and $s2$. When M reaches its maximum value, a template can be generated in the 0 °, 45 °, 90 °, 135 °, 180 °, 225 °, 270 °, and 315 ° counterclockwise directions at this point, as shown in Figure 2. According to equation (1), the gray distribution difference in the neighborhood of a pixel can be calculated to further obtain the direction information of the point. When there is a direction line passing through an area, if the template can make equation (1) get the maximum value, it means that the difference of pixel gray distribution on both sides of the direction line is the largest. The explanatory equation (1) can reflect the direction information of pixel points.

There is a certain degree of correlation and correlation between the pixels in the image, and the correlation between
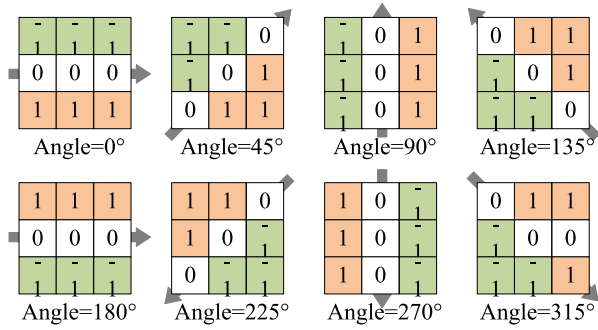
FIGURE 2. Display of eight direction information templates for image blocks.

the points closest to the specified pixels is more significant. This correlation also exists between image blocks composed of several pixel points. The Structural Similarity Index Measurement (SSIM) indicator is currently widely utilized in image quality evaluation. It can divide the information of an image into brightness, contrast, etc. from the perspective of image structure, and the division is relatively independent, which can accurately reflect the attributes of the object structure in the image. SSIM indicators can be combined to model image structure, brightness, and contrast, using the mean, standard deviation, and covariance of pixel grayscale values to evaluate the brightness, contrast, and structural similarity of the image. Therefore, SSIM can be used to evaluate the similarity between image blocks,which increases the robustness of image block similarity indicators. Assuming that there are image blocks x and y in the image to be processed, and the size of both image blocks is $N \times N$, the brightness $l(x, y)$ of these two image blocks in SSIM can be expressed according to equation (2).

$$l(x, y) = \left(2\mu_x\mu_y + C_1\right) \Big/ \left(\mu_x^2 + \mu_y^2 + C_1\right) \qquad (2)$$

In equation (2), C_1, C_2, and C_3 are all small positive numbers to prevent the equation from having a denominator of zero; μ_x and μ_y serves as the pixel mean of the corresponding image block. The contrast $c(x, y)$ between two image blocks can be calculated according to equation (3).

$$c(x, y) = \left(2\sigma_x\sigma_y + C_2\right) \Big/ \left(\sigma_x^2 + \sigma_y^2 + C_2\right) \qquad (3)$$

In equation (3), σ_x and σ_x represent the pixel standard deviation of the corresponding image block. The covariance $s(x, y)$ of two image blocks can be calculated according to equation (4).

$$s(x, y) = \left(\sigma_{xy} + C_3\right) \Big/ \left(\sigma_x\sigma_y + C_3\right) \qquad (4)$$

In equation (4), σ_{xy} represents the covariance μ_x and μ_y of two image blocks, which are calculated using the same method as in equation (5).

$$\mu_x = \frac{\sum\limits_{i=1}^{N} x_i}{N} \qquad (5)$$

The calculation method for σ_x and σ_x is the same, refer to equation (6).

$$\sigma_x^2 = \frac{\sum\limits_{i=1}^{N} (x_i - \mu_x)^2}{N - 1} \qquad (6)$$

The calculation method for σ_{xy} is shown in equation (7).

$$\sigma_{xy} = \frac{\sum\limits_{i=1}^{N} (x_i - \mu_x)\left(y_i - \mu_y\right)}{N - 1} \qquad (7)$$

The SSIM model $SSIM(x, y)$ can be obtained by combining equations (2), (3), and (4), as shown in equation (8).

$$SSIM(x, y) = \frac{\left(2\mu_x\mu_y + C_1\right)\left(2\sigma_{xy} + C_2\right)}{\left(\mu_x^2 + \mu_y^2 + C_1\right)\left(\sigma_x^2 + \sigma_y^2 + C_2\right)} \qquad (8)$$

Although the $SSIM(x, y)$ model can reflect the geometric similarity between image blocks, all the data involved in the calculation are pixel grayscale values, lacking directional structural information of the image blocks. And this type of information can reflect more features of the image, making the similarity calculation more accurate. Now it adds directional information to it and obtains $SSIM(x, y)'$ as shown in equation (9).

$$SSIM(x, y)' = \frac{\left(2\mu_x\mu_y + C_1\right)\left(2\sigma_{xy} + C_2\right)S}{\left(\mu_x^2 + \mu_y^2 + C_1\right)\left(\sigma_x^2 + \sigma_y^2 + C_2\right)N} \qquad (9)$$

In equation (9), S is the total number of pixels with the same directional information in two image blocks. According to equation (9), an indicator that can relatively accurately describe image block information can be calculated. In the traditional NLM algorithm, the range of Gaussian weighted Euclidean distance values is [1, 0]. The higher the numerical value, the higher the similarity in the two objects. However, the range of $SSIM(x, y)'$ values is not consistent with the former, which is [1, -1]. The larger the $SSIM(x, y)'$ value, the higher the similarity. To fuse $SSIM(x, y)'$ with Gaussian weighted Euclidean distance, it is necessary to modify the definition of the former. The modified model $LS(x, y)$ is shown in equation (10).

$$LS(x, y) = \frac{1 - SSIM(x, y)'}{2} \qquad (10)$$

The model of equation (10) includes the degree of similarity of the directional geometric information between two image blocks, which is referred to here as the directional structural similarity parameter. To further demonstrate the contribution of image blocks to the denoising effect, it is necessary to normalize $LS(x, y)$. By multiplying the Gaussian-weighted Euclidean distance with the directional structure similarity parameter can obtain the final improved adjacent image block similarity index. The calculation method is shown in equation (11).

$$d(x, y)' = \left\| v(N_x) - v(N_y) \right\|_{2,\alpha}^2 \cdot LS(x, y)' \qquad (11)$$

In equation (11), $LS(x,y)'$ is the similarity of the directional structure of the normalized image blocks; N_x and N_y represents the quantity of pixels in the corresponding direction within the image block; $v()$ is a Gaussian weighting function for the number of pixels; α is the distance calculation parameter. In summary, the NLM calculation process based on the improved similarity calculation method can be expressed in Figure 3.
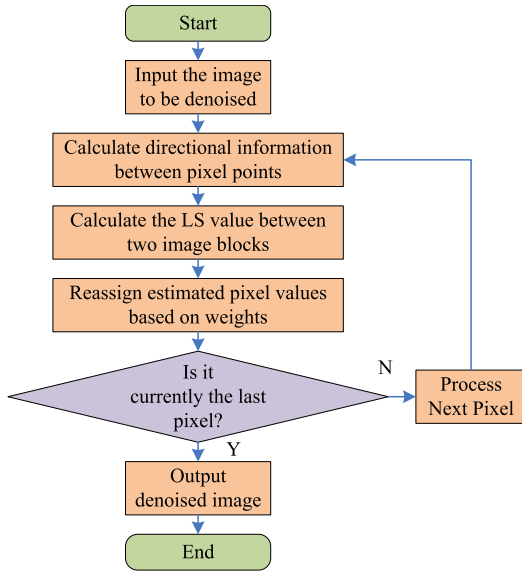

FIGURE 3. NLM calculation process based on improved similarity calculation method.

B. IMPROVED IMAGE EDGE DETECTION METHOD BASED ON CANNY OPERATOR

In the NLM algorithm, the filtering similarity weight parameter h has a significant impact on the denoising results. If this parameter is set too large, the denoised image will become more blurry and lose more non noise information. On the contrary, if the h parameter is set too small, it will not achieve good denoising effect. The setting of visible parameter h requires consideration of noise level factors. Previous studies have mostly used a globally fixed method to determine parameter h, which is simple to set, but the disadvantage is that the overall unified parameters cannot be intelligently adjusted according to the specific denoising image structure and noise situation. For images with significant differences in local noise situations, this method has poor denoising effect. Therefore, this parameter should have a certain degree of adaptability, and the corresponding parameter values can be determined based on the specific image content. The prerequisite for completing this step is to reasonably distinguish the content structure in the image. Considering that the main difference between flat and dense areas in an image is the difference in grayscale values. In areas with abundant information, the grayscale changes are more significant, and the areas with the most significant grayscale changes are mostly located at the edges of the image. In flat areas of the image,

the grayscale value changes more slowly, and these changes often do not occur at the edges of the image. That is to say, it is possible to identify whether the image is a region with rich details by extracting image edges, in preparation for setting adaptive h parameter adjustment mode in the future.

The edge detection algorithm for grayscale images utilizes gradients to reflect the magnitude and direction of grayscale changes, and uses gradient amplitude thresholding to extract image edges. The edge detection algorithms for grayscale images can be divided into first-order and second-order differential image edge detection algorithms. The first order differential image edge detection algorithms include Krisch, Roberts, Sobel, Prewitt, and others. The Prewitt algorithm is widely used, and its calculation template is shown in Figure 4. In this algorithm, pixels with grayscale values less than the threshold are not considered edge points, and this judgment method is not reasonable enough. Because noise can cause some pixels to have larger grayscale values, this algorithm misjudges them as variable edge points, while other edge points are relatively weak and may be lost.
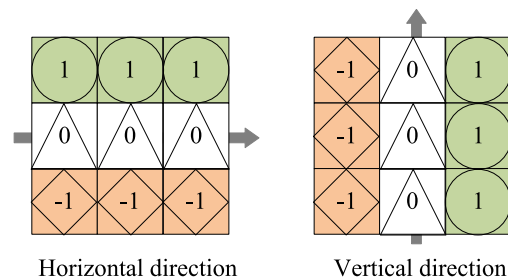

FIGURE 4. Presentation of the calculation method of the Prewitt operator.

The Sobel algorithm in first-order differential image edge detection has the low computational complexity and high edge detection efficiency, and is also widely used in various scenarios. It is particularly suitable for situations with low precision requirements for fine texture processing. Its computational model is shown in Figure 5.
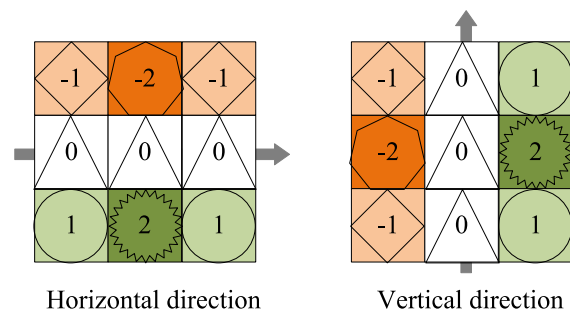

FIGURE 5. Display of Sobel operator calculation method.

The difference between different edge detection operators lies in the different templates used to calculate the vertical and horizontal gradient components of the image. Meanwhile, the gradient calculation method is simple and sensitive to noise, especially susceptible to pulse noise. Therefore, the difficulty

of selecting the gradient threshold for the one-dimensional differential image edge detection algorithm is high, and the detected edges have no pixel width. The edge position of the image in the two-dimensional differential image edge detection algorithm is determined by the extreme value or zero intersection of the second-order direction reciprocal. Canny is a typical two-dimensional differential image edge detection algorithm. Its main advantage over other operators is that it is not easily affected by noise and can accurately detect weak edges. Therefore, this study chose this operator for edge detection calculation. The main calculation steps of canny operatorare detection, enhancement, and filtering. The main performance evaluation indicators of the Canny algorithm include thesignal-to-noise ratio, the positioning accuracy, and the average distance of the zero intersection points in the pulse response of the detection algorithm. In this study, the Canny algorithm is used for image edge detection to distinguish flat areas from information-rich areas in the image. The main extraction steps are as follows: The first step is image filtering, which uses a two-dimensional Gaussian template for performing convolution calculation with the original image to eliminate noise interference in the detection. The second step is to calculate the gradient direction and assignment. Canny algorithm utilizes the finite difference of the first order partial derivative of the 2 * 2 neighborhood for calculating the gradient direction and corresponding amplitude of the smoothed image $V(x, y)$. The gradient amplitude $G(x, y)$ calculation method is shown in equation (12).

$$G(x, y) = \sqrt{g_x^2(x, y) + g_y^2(x, y)} \qquad (12)$$

$g_x(x, y)$ and $g_y(x, y)$ represents the first order directional partial derivative of $V(x, y)$ in two directions respectively. The direction $\theta(x, y)$ of $V(x, y)$ is calculated according to equation (13).

$$\theta(x, y) = \arctan\left(\frac{g_y(x, y)}{g_x(x, y)}\right) \qquad (13)$$

The final step in the Canny algorithm is to suppress non maximum values in gradient images. The gradient amplitude matrix element corresponding to the image is directly proportional to the gradient value of the point, but relying solely on this relationship is not enough to determine whether a point is an edge point. It is also necessary to consider the current position and the gradient values on both sides during the comparison process. If the gradient value of the current position is less than the gradient of either side, set the pixel value of that point to 0. Moreover, it is necessary to compare the intersection value of the gradient direction at this point. If the gradient value at this point is less than the latter, it is considered that this point is not a maximum point. The final step of the Canny algorithm is dual threshold detection and edge connection processing. The image is transformed into binary form after non maximum suppression processing, where the pixel values at the edge and non edge pixels are labeled as 1 and 0, respectively. But at this point, the image still contains a lot of noise, and it is necessary to further combine double threshold detection and edge connection processing. The essence of dual threshold processing is to select a high threshold to reduce false edges in the image. In summary, the process of selecting theCanny algorithm for image edge detection is shown in Figure 6.
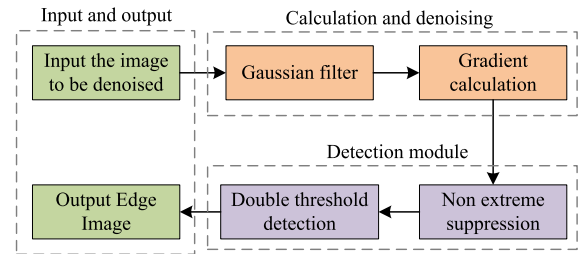

FIGURE 6. Canny algorithm calculation process.

After using the Canny algorithm to distinguish image regions, edge pixels can be accurately recorded. In areas with complex edges, the image is detected with more edge pixels, while in areas with simple edges, fewer pixels are detected. By counting the data of edge pixels in the detected area, the richness of the detailed structure of the area can be determined, which in turn determines the size of the filter parameters. Therefore, the adaptive filtering parameter h.

$$h = \sigma \times k \qquad (14)$$

In equation (14), σ is the noise variance; k is the variable coefficient. h is determined by two parameters, σ and k. It sets the total number of pixels within the search range to N and the number of edge pixels to S. Then, according to the size of S/N, the level of detail information richness in the region can be determined. Based on the actual situation of ID work, the value of k is set in the form of equation (15).

$$k = \begin{cases} 18, & S/N = 0 \\ 12, & 0 < S/N < 0.3 \\ 10, & 0.3 < S/N < 0.7 \\ 8, & S/N > 0.7 \end{cases} \qquad (15)$$

By using equation (15), h can be adjusted based on the region information of the image. When the number of edge pixels in the search area is large, it indicates that the region has more detailed information, and the corresponding k value will be smaller. Conversely, the value of k will be larger. When the number of pixels at the edge of the search area is zero, it indicates that this is a flat area, and k is taken as the maximum value. It can be seen that the filtering parameter J will be adjusted according to different k values, resulting in adaptability. At this point, the NLM algorithm that integrates the improved direction structure information and adaptive filtering parameters has been designed, and the overall calculation process is shown in Figure 7.

Finally, considering the poor ability of NLM algorithm to mine the similarity between image blocks, this paper proposes to integrate neural network structure in NLM
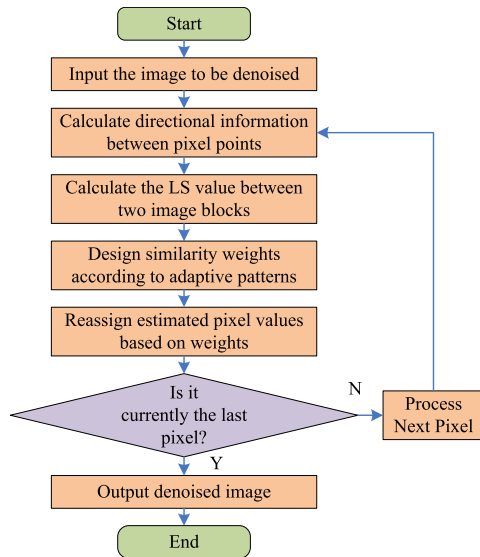
FIGURE 7. NLM calculation process based on improved similarity calculation method.

FIGURE 8. Technical route and complete process demonstration of denoising research.

algorithm, and use the latter to find and optimize the mapping function between image blocks to assist NLM algorithm in finding the similarity between image blocks. Considering the size and scale of the input data for this study, a neural network consisting of five layers is constructed, namely input layer, hidden layer 1, hidden layer 2, hidden layer 3, and output layer. The corresponding number of neurons is 64, 512, 512, 512, 64, and the image block is divided into 8 layers × Size of 8. This neural network structure selects ReLU function as the Activation function, selects the mean square logarithm error to construct the Loss function, and uses L2 regularization term. Therefore, the overall calculation process of the denoising model after adding a neural network structure is as follows: the NLM algorithm processes the weights between two image blocks (considered as similar blocks and reference blocks respectively), multiplies this weight with each pixel in the base block to obtain an output of the same size, and serves as the input for the neural network structure in the model; The neural network structure will output the optimal mapping function between image blocks for subsequent denoising calculations in the NLM algorithm. So far, the Technology roadmap of this research can be obtained, as shown in Figure 8.

IV. PERFORMANCE TESTING OF IMPROVED NON LOCAL MEAN IMAGE DENOISING ALGORITHM

To compare and analyze the application value and effectiveness of the improved NLM algorithm (INLM) designed in this study in the field of ID, and to provide reference for the market application of this algorithm, a denoising experiment needs to be designed and conducted now.

A. EXPERIMENTAL PLAN DESIGN

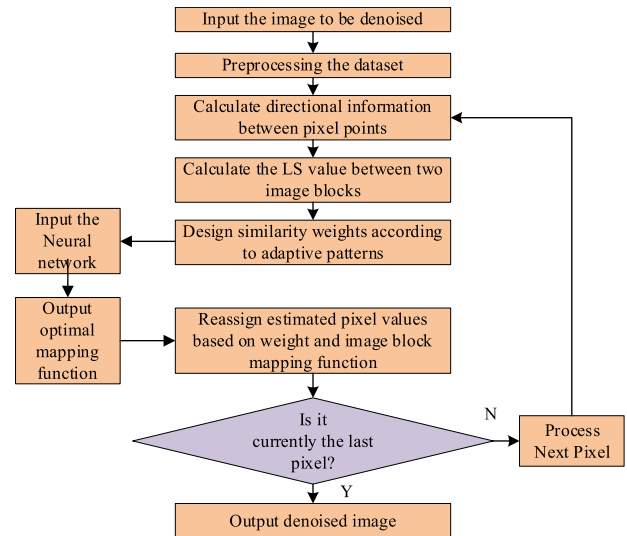In the experiment, traditional NLM, Median filtering (MF), and Generative Adversarial Networks (GAN) were selected

to construct a contrastive denoising model. The parameters of the GAN denoising model are determined using the binary debugging method. To improve the reliability of the denoising results as much as possible, several common denoising datasets were selected in this study to participate in the experiment. The specific information and particularsis indicated in Table 1. As shown in Table 1, the selected datasets all have rich image scenes, with a large number of image groups and almost different image types. At the same time, all datasets contain test sets. These situations indicate that the selected dataset can meet the experimental requirements and fully validate the denoising performance of the designed algorithm in different scenarios and conditions. In addition, in the experiment, the denoising model and all contrast denoising models designed in this research were built using the Python programming language. The operating platform and environment of the experiment are as follows: the operating system is Windows10 Professional Edition, the host processor Intel Core i7, the size of Random-access memory is 6GB, and the size of read-only memory is 1024G.

For denoising models that require training, such as GAN models, the entire dataset data is scrambled and divided into a test set and training set in a 3:7 ratio for model training and testing. In the experiment, information entropy (IE) IE, Peak Signal to Noise Ratio (PSNR), Average gradient (AG), Structural Similarity (SSIM), mutual information (MI), Root mean square error (RMSE), and absolute error (MAE) were selected to evaluate the denoising effect.Among them, IE, AG, SSIM, and MI can also serve as metrics to measure the information loss of denoised images relative to non-noised images. These selected indicators can objectively and consistently compare the denoising performance of different denoising algorithms, as well as the ability to retain original non noise information without being influenced by subjective opinions [23].

IEEE *Access*

L. Shi: Geometric Structure Based Non Local Mean Image Denoising Algorithm

TABLE 1. Basic information statistics of denoising experiments.

Number	Name	Number Of Scenes	Number Of Images (Group)	Number Of Camera Types	Type	With Or Without Training Set
#01	Renior	120	240	3	Low Light	Have
#02	Nam-Cc15	11	17	3	Goods	Have
#03	Nam-Cc60	11	60	3	Goods	Have
#04	Polyu	40	40	5	Indoor And Outdoor	Have
#05	Sidd	200	400	5	Multi Domain	Have
#06	High-Iso	28	110	4	High Sensitivity	Have
#07	Nind	101	606	2	Multi-Level Sensitivity	Have

B. ANALYSIS OF IMAGE DENOISING QUALITY

After the experiment is completed, the quality of the denoised image is analyzed first. The IE of the denoised image using the various models is shown in Figure 10. The horizontal axis in Figures 9 to 13 represents the noise variance, while the vertical axis represents the evaluation indicators corresponding to the normalized image after denoising. Different line styles represent different denoising models. Figure 9 shows that there is an overall negative correlation between the denoised image IE and the noise variance of all denoising models. However, for any identical noise variance value, the INLM algorithm designed in this study has a higher IE than the NLM algorithm before improvement, and also higher than other denoising algorithms. When the noise variance is 25, the normalized IE of INLM, NLM, MF, and GAN are 0.58, 0.51, 0.46, and 0.56, respectively. At this point, the normalized IE values of references [21] and [22] are 0.49 and 0.53, respectively. This is because the improved NLM algorithm proposed in reference [21] considers more pixels for denoising compared to traditional NLM algorithms, and the denoising effect is better. However, the improved NLM algorithm designed in reference [22] determines the important points of the reference points around the denoised points in a non equal weight manner, and the denoising effect is better than that in reference [21], but it still fails to take into account the directional structure information of the image, Therefore, the denoising effect is inferior to the algorithm designed in this study.

The PSNR values of the various denoised models are shown in Figure 10. In Figure 10, the HA represents the noise variance, and the VA represents the PSNR of the denoised image after normalization. Figure 10 illustrates that with the increase of noise variance, the information entropy of the denoised image of all denoising models shows a downward trend. However, for any identical noise variance value, the PSNR of the denoised image designed by the INLM algorithm in this study exceeds that of the improved NLM algorithm, and is also superior toother denoising algorithms. For example, when the noise variance is 25, the normalized PSNR of INLM, NLM, MF, and GAN are 0.62, 0.51, 0.45, and 0.57, respectively.The normalized PSNR of the denoising models in references [21] and [22] are 0.47 and 0.59 when
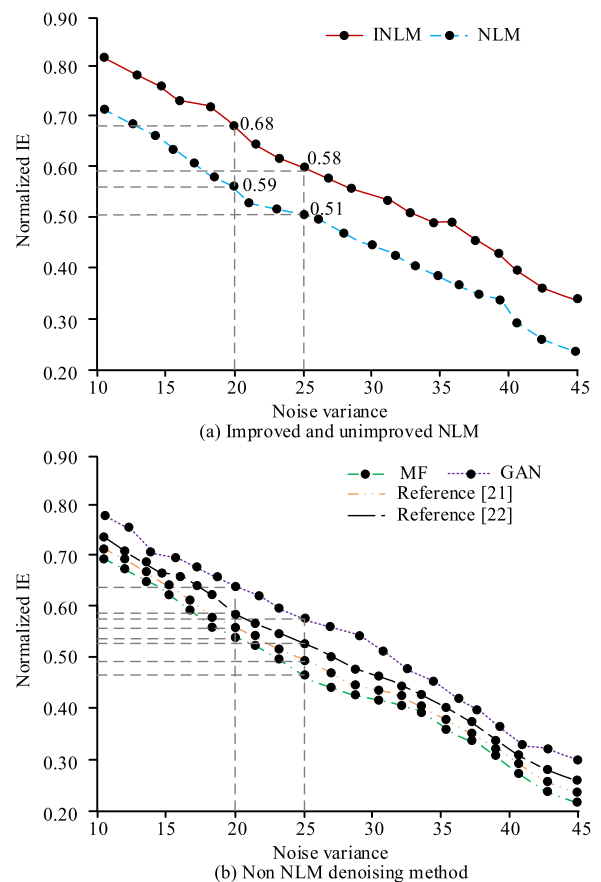

(a) Improved and unimproved NLM

(b) Non NLM denoising method

FIGURE 9. IE of four models for denoised images under different noise variances.

the noise variance is 25, respectively, because neither method takes into account the directional structure information that has a significant impact on the denoising effect, and the method in reference [21] requires a large number of adjacent pixels to obtain good processing results.

As PSNR is a core indicator for evaluating the denoising ability of denoising methods, in order to further improve the reliability of comparison results. Here, we also selected the novel and advanced denoising algorithm currently on the market, namely Noise2Noise proposed in 2018, and the Flexible

91152

VOLUME 11, 2023

and Fast Denoising Convolutional Neural Network (FFDNet) proposed in 2018 for comparative experiments. Similarly, the normalized PSNR of Noise2Noise and FFDNet is still lower than that of INLM under various noise variance conditions.
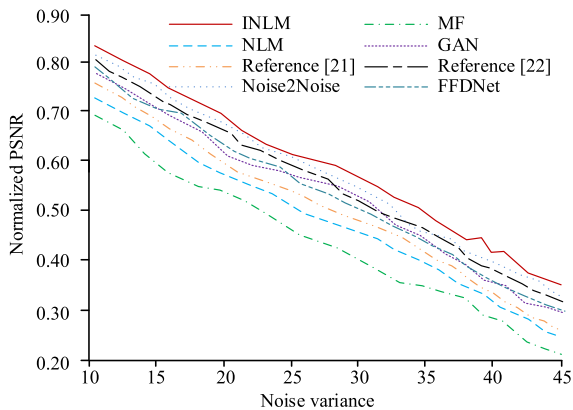

FIGURE 10. PSNR of six models for denoised images under different noise variances.

Then, the AG index was then used to evaluate the image quality of each model after denoising, and the statistical results are demonstrated in Figure 11. Each noise scheme was repeated 5 times, and the mean and standard deviation of the normalized AG values were calculated and marked in Figure 11. The dashed lines corresponding to each color icon in the figure represent the trend-fit curve of the series of data changes. Figure 11 shows that the smaller the noise variance, the larger the AG value of the output images of each denoising model; This indicates that the better the quality of the ID, the richer the information retained in the denoised image. After the noise variance increases, the AG values of the output images of each denoising model begin to decrease. When the noise variance is 50, the AG values of each model reach the minimum, and the normalized AG means of INLM, NLM, MF, and GAN are 0.43, 0.29, 0.28, and 0.33, respectively. This indicates that the image information richness processed by the INLM denoising algorithm designed in the study is still the highest, while the differences in the image information richness processed by the other three algorithms are relatively small.

C. CORRELATION ANALYSIS BETWEEN DENOISED IMAGES AND NOISELESS IMAGES

From the perspectives of SSIM, MI, RMSE, and MAE, the correlation between the denoised images of each model and the original image without noise is compared. The performance of the denoised images of each model on SSIM is shown in Figure 12. The HA in Figure 12 serves as the noise variance, while the VAserves as the SSIM values after denoising and image normalization. The gray short dashed line represents the trend fitting line of the corresponding line segment. Figure 12 shows that there is an overall negative correlation between the information entropy of the denoised image and the noise variance of all denoising models.
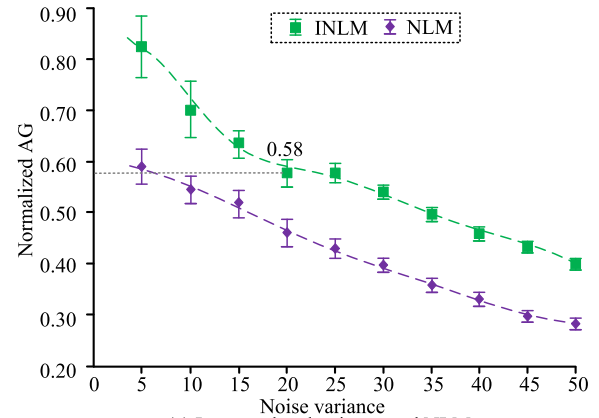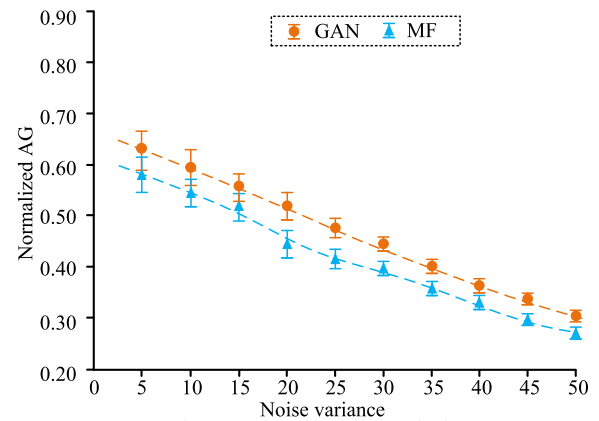
FIGURE 11. AG of denoised images for each model under different noise variances.

However, when the noise variance values are equal, the SSIM of the INLM algorithm outperforms all other denoising models. For example, when the noise variance is 45, the normalized SSIM of INLM, NLM, MF, and GAN are 0.88, 0.56, 0.61, and 0.82, respectively, At this point, the normalized SSIM values for references [21] and [22] are 0.73 and 0.80, respectively, which are both smaller than the designed denoising algorithm INLM.

It further analyzes the degree to which the denoised images of the four models retain the information of the original noiseless images, and the statistical results are indicated in Figure 12. In Figure 12, the HA serves as the noise variance, and the VA serves as the MI after image normalization after denoising; Sub graph (a) is used to compare the improved NLM algorithms before and after improvement, while sub graph (b) is used to compare non NLM denoising algorithms. A linear model was used to fit the normalized MI noise variance data of each denoising algorithm, and the optimal fitting results were added in a line segment manner to Figure 13. Figure 13 demonstrates that as the noise variance increases, the MI of the denoised images of all denoising models begins to fluctuate and increase. Overall, the INLM algorithm has the best MI data stability. In the absence of repeated data fluctuations and with the same noise variance, the numerical value
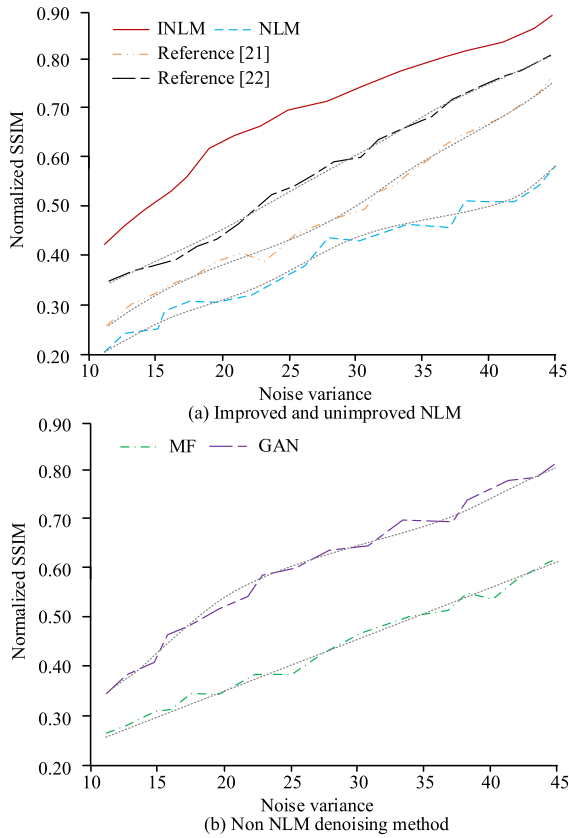
FIGURE 12. SSIM of denoised images for each model under different noise variances.

FIGURE 13. MI of denoised images for each model under different noise variances.

is always greater than that of the other algorithms. When the noise variance is small, the MI of the GAN model denoised image is lower than that of the MF algorithm; When the noise variance exceeds 23, the relative size relationship between the two is reversed. For example, when the noise variance is 45, the normalized MI of INLM, NLM, MF, and GAN are 0.78, 0.52, 0.55, and 0.74, respectively.

The RMSE and MAE values of the four denoised models are shown in Figure 14. The HA in Figure 14 serves as the denoising calculation and evaluation indicators, the left VA is used to display the EMSE of the denoised image, the right VA is used to display the MAE of the denoised image, and different box fill colors represent different evaluation indicators. Figure 14 shows that the RMSE and MAE values of the INLM denoising algorithm designed for this study are significantly lower than the other three algorithms, regardless of the classification of the noise error data. Among the other three algorithms, the unmodified NLM algorithm has the highest RMSE and MAE values of the denoised image. Because the median normalized RMSE and MAE for INLM, NLM, MF, and GAN are 8.2, 19.6, 18.5, 17.1, and 9.7, 21.4, 18.0, and 18.2, respectively.

The above data indicates that the INLM denoising algorithm designed in this study has the most original noise-less image information after denoising, and has the best
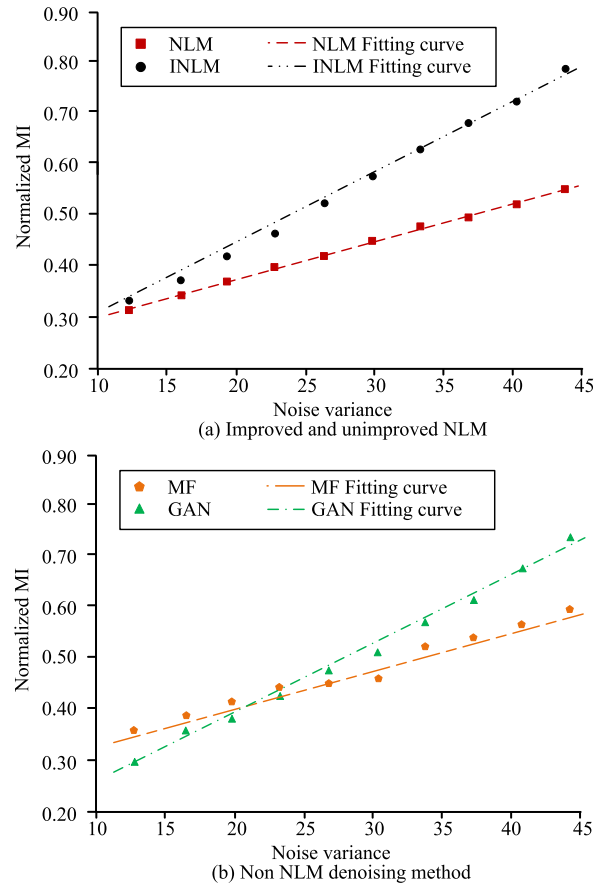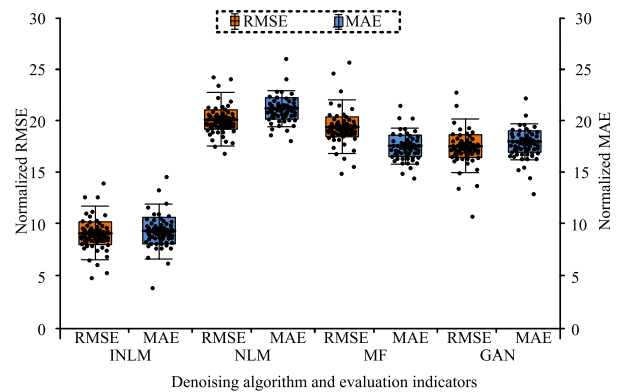

FIGURE 14. Denoised images RMSE and MAE of four models.

overall and structural similarity with the original noiseless image. Moreover, the improvement level is significantly different from traditional NLM denoising algorithms.

Finally, the performance of each algorithm is compared from the perspective of the computational efficiency of the algorithms themselves. The chosen comparison indicator is the computation time, measured in milliseconds. The statistical results are demonstrated in Table 2. Table 2 indicates that from the perspective of average computing time, the INLM

TABLE 2. Comparison of calculation time for various denoising models.

Number of denoised image groups	Average denoising time/ms				Maximum denoising time/ms			
	INLM	NLM	MF	GAN	INLM	NLM	MF	GAN
300	69	37	39	114	78	43	41	195
600	137	71	68	225	148	79	75	327
900	208	110	105	329	225	114	118	514
1200	274	143	132	426	306	156	152	781
1473	316	183	172	523	351	195	188	906

algorithm designed in this study does not have the smallest denoising time, higher than the NLM and MF algorithms, but the GAN algorithm has the highest average computing time. From the perspective of maximum computing time, the difference in maximum computing time between MF and NLM algorithms is small, while the maximum computing time of INLM algorithm is still only smaller than GAN. The maximum calculation time of GAN increases significantly compared to the average calculation time under the same conditions, mainly due to the complex structure of the trained GAN neural network and the large number of calculation parameters. Therefore, the calculation time is also greater than other algorithms. The main reason why the calculation time of the INLM algorithm designed in this study exceeds that of traditional NLM algorithm is that the latter has a simpler similarity calculation method, does not need to consider the direction information of square image blocks, and does not require the use of Canny operator for image edge point detection. Therefore, the computational complexity is lower. When the number of contemporary denoised image groups is the whole data set, the average calculation time for INLM, NLM, MF, and GAN is 316ms, 183ms, 172ms, and 523ms, respectively.

Due to the commonality and harm of Gaussian noise, denoising tests are now conducted separately for this type of noise. 2688 images containing Gaussian noise were selected from the dataset for denoising comparison experiments. The experimental results showed that the INLM algorithm designed in this study had normalized IE and normalized SSIM values of 0.69 and 0.65, respectively, under the condition of noise variance of 20, which were still higher than all comparison models. The processing effect of Gaussian noise in this model is also relatively good. The main reason for this phenomenon is that the designed model has both a neural network structure and an improved NLM module. Its ability to extract local and global information from images is stronger, and it is less susceptible to noise and loss of non noise information.

V. CONCLUSION
To address the issue of image denoising, we are now improving the NLM algorithm. In the study, NLM, MF, GAN algorithms, as well as algorithms from references [21] and [22], were also selected for denoising experiments based on various common noisy image standard datasets. After the experiment, it was found that when the noise variance was 25,

the normalized PSNR of INLM, NLM, MF, GAN algorithm, reference [21] method, and reference [22] method were 0.62, 0.51, 0.45, 0.57, 0.47, and 0.59, respectively. The denoising effect of the INLM denoising algorithm designed in this study is significantly better than the comparison algorithm and the traditional NLM algorithm before improvement. From the perspective of preserving the original noiseless image information, the INLM algorithm performs better than other algorithms in SSIM, MI, RMSE, and MAE. When the noise variance is 45, the normalized SSIM of INLM, NLM, MF, GAN, reference [21] method, and reference [22] method are 0.88, 0.56, 0.61, 0.82, 0.73, and 0.78, respectively. It can be seen that the image denoised by INLM algorithm has the most original noiseless image information and the denoising effect is significantly better. The results of this study can provide image and video processing methods with better denoising performance for meteorological prediction, emergency search and rescue, and other fields. However, due to research time constraints, the improved algorithm was not deployed for testing in market products, which also pointed out the direction for future research.

REFERENCES
[1] Y. Zhu, X. Pan, T. Lv, Y. Liu, and L. Li, "DESN: An unsupervised MR image denoising network with deep image prior," *Theor. Comput. Sci.*, vol. 880, no. 3, pp. 97–110, Aug. 2021.

[2] C. Tian, Y. Xu, W. Zuo, B. Du, C.-W. Lin, and D. Zhang, "Designing and training of a dual CNN for image denoising," *Knowl.-Based Syst.*, vol. 226, Aug. 2021, Art. no. 106949.

[3] S. Wang, K. Xia, L. Wang, J. Zhang, and H. Yang, "Improved RPCA method via non-convex regularisation for image denoising," *IET Signal Process.*, vol. 14, no. 5, pp. 269–277, Jul. 2020, doi: 10.1049/iet-spr.2019.0365.

[4] H. Deng, J. Tao, X. Song, and C. Zhang, "Estimation of the parameters of a weighted nuclear norm model and its application in image denoising," *Inf. Sci.*, vol. 528, pp. 246–264, Aug. 2020, doi: 10.1016/j.ins.2020.04.028.

[5] Y. Su, Z. Li, H. Yu, and Z. Wang, "Multi-band weighted l_p norm minimization for image denoising," *Inf. Sci.*, vol. 537, pp. 162–183, Oct. 2020, doi: 10.1016/j.ins.2020.05.049.

[6] H. Xia, F. Zhu, H. Li, S. Song, and X. Mou, "Combination of multiscale and residual learning in deep CNN for image denoising," *IET Image Process.*, vol. 14, no. 10, pp. 2013–2019, Jul. 2020.

[7] S. Lee, M. Negishi, H. Urakubo, H. Kasai, and S. Ishii, "Mu-net: Multiscale U-net for two-photon microscopy image denoising and restoration," *Neural Netw.*, vol. 125, pp. 92–103, May 2020.

[8] J. Ji, J. Wei, G. Fan, M. Bai, J. Huang, and Q. Miao, "Image patch prior learning based on random neighbourhood resampling for image denoising," *IET Image Process.*, vol. 14, no. 5, pp. 838–844, Apr. 2020.

[9] H. Ye, H. Li, and C. L. P. Chen, "Adaptive deep cascade broad learning system and its application in image denoising," *IEEE Trans. Cybern.*, vol. 51, no. 9, pp. 4450–4463, Sep. 2021.

[10] K. Li, W. Zhou, H. Li, and M. A. Anastasio, "Assessing the impact of deep neural network-based image denoising on binary signal detection tasks," *IEEE Trans. Med. Imag.*, vol. 40, no. 9, pp. 2295–2305, Sep. 2021.

[11] P. Li, H. Wang, X. Li, and C. Zhang, "An image denoising algorithm based on adaptive clustering and singular value decomposition," *IET Image Process.*, vol. 15, no. 3, pp. 598–614, Feb. 2021.

[12] H. Golshan and R. P. R. Hasanzadeh, "Fuzzy hysteresis smoothing: A new approach for image denoising," *IEEE Trans. Fuzzy Syst.*, vol. 29, no. 3, pp. 686–697, Mar. 2021.

[13] P. Jia, X. Li, Z. Li, W. Wang, and D. Cai, "Point spread function modelling for wide-field small-aperture telescopes with a denoising autoencoder," *Monthly Notices Roy. Astronomical Soc.*, vol. 493, no. 1, pp. 651–660, Jan. 2020.

[14] Y. Lotfi and K. Parand, "Efficient image denoising technique using the meshless method: Investigation of operator splitting RBF collocation method for two anisotropic diffusion-based PDEs," *Comput. Math. Appl.*, vol. 113, pp. 315–331, May 2022.

[15] Riya, B. Gupta, and S. S. Lamba, "An efficient anisotropic diffusion model for image denoising with edge preservation," *Comput. Math. Appl.*, vol. 93, pp. 106–119, Jul. 2021.

[16] L. Han, S. Li, and X. Liu, "Image denoising based on BCOLTA: Dataset and study," *IET Image Process.*, vol. 15, no. 3, pp. 624–633, Feb. 2021.

[17] Q. Xiang, L. Peng, and X. Pang, "Image denoising auto-encoders based on residual entropy maximum," *IET Image Process.*, vol. 14, no. 6, pp. 1164–1169, May 2020.

[18] C. Tian, L. Fei, W. Zheng, Y. Xu, W. Zuo, and C.-W. Lin, "Deep learning on image denoising: An overview," *Neural Netw.*, vol. 131, pp. 251–275, Nov. 2020.

[19] Y. Yang and X. Song, "Research on face intelligent perception technology integrating deep learning under different illumination intensities," *J. Comput. Cognit. Eng.*, vol. 1, no. 1, pp. 32–36, Jan. 2022.

[20] Y. Lei, "Research on microvideo character perception and recognition based on target detection technology," *J. Comput. Cognit. Eng.*, vol. 1, no. 2, pp. 83–87, Jan. 2022.

[21] A. Buades, B. Coll, and J.-M. Morel, "A non-local algorithm for image denoising," in *Proc. IEEE Comput. Soc. Conf. Comput. Vis. Pattern Recognit. (CVPR)*, Jun. 2005, pp. 60–65, doi: 10.1109/CVPR.2005.38.

[22] J.-R. Liao and C. Y. Chan, "Efficient implementation of non-local means image denoising algorithm," in *Proc. IEEE 8th Global Conf. Consum. Electron. (GCCE)*, Osaka, Japan, Oct. 2019, pp. 566–567, doi: 10.1109/GCCE46687.2019.9015454.

[23] Y. Ou, J. Luo, B. Li, and M. N. S. Swamy, "Gray-level image denoising with an improved weighted sparse coding," *J. Vis. Commun. Image Represent.*, vol. 72, no. 3, Oct. 2020, Art. no. 102895, doi: 10.1016/j.jvcir.2020.102895.

LEI SHI was born in Hulunbuir, Inner Mongolia, China, in 1982. He received the master's degree from the Harbin Institute of Technology, China, in 2013. Since 2006, he has been with the School of Mathematics and Physics, Hulunbuir University. He has authored one book, seven articles, and owns four software copyrights. His research interests include image processing, applied mathematics, and mathematics education.

● ● ●